Chemoselective nickel-catalyzed coupling through substrate photoexcitation

Pradipta Das,[a] Eliot F. Woods,[a] Jack T. Ly,[b,c] Jack N. Olding,[d] Kayla F. Presley,[b,c] Brennan Romanoff,[e] Tod A. Grusenmeyer,[b] Emily A. Weiss,[a,d,f] and Julia A. Kalow*[a]

ABSTRACT: Metallaphotoredox catalysis combines the well-established mechanisms of transition-metal-catalyzed cross-coupling reactions with one-electron redox manipulations enabled by light. In most cases, a transition metal or organic dye serves as the photoredox catalyst while a ground-state Pd or Ni catalyst performs the organometallic steps. Cross-coupling mechanisms that rely on direct photoexcitation of a light-absorbing substrate have the potential to access distinct mechanisms and deliver unique selectivity based on the substrate's excited-state properties. In this report, we describe a photoinduced, Ni-catalyzed Suzuki–Miyaura cross coupling reaction that selectively functionalizes BODIPY chromophores, a versatile class of tunable, bright, photostable fluorophores. Using a bis-iodo BODIPY substrate, the selectivity for mono- vs. bis-arylation was found to be governed by a remote substituent that subtly alters the excited-state properties of the substrate. Consistent with a substrate photoexcitation mechanism, high chemoselectivity is also observed in mixtures of chromophores with distinct excited-state properties. This reaction is compatible with a variety of substituted BODIPY chromophores and boronic acids and esters, enabling the rapid synthesis of unsymmetrically-substituted chromophores.

INTRODUCTION

The introduction of light to transition-metal-catalyzed cross-coupling reactions has enabled new transformations and accelerated known reactions of challenging substrates.[1] In metallaphotoredox catalysis, a photoredox catalyst engages in single-electron transfer (SET) with the substrate and/or transition-metal cocatalyst to generate radical intermediates or change oxidation states, respectively. More recently, many examples of light-driven cross-coupling reactions *without* a photoredox catalyst have been reported (Figure 1).[2–7] The proposed role of light is direct photoexcitation of a catalyst such as Pd(0), which significantly lowers the barrier for oxidative addition by accessing one-electron mechanisms or facilitating challenging reductive eliminations (**Figure 1a**).[8] While photoexcitation of a catalyst—be it a photoredox catalyst or a low-valent Pd or Ni catalyst—can activate it towards SET with a ground-state aryl halide substrate,[9–11] in principle, photoexcitation of the organic substrate should also induce SET with a ground-state catalyst. However, typical organic substrates do not absorb visible light, so previous approaches that employ substrate photoexcitation rely on deprotonation (**Figure 1b**)[2,4] or electron donor-acceptor (EDA) complexation (**Figure 1c**)[12,13] to induce reactivity. We envisioned that direct substrate photoexcitation could enable the selective functionalization of organic chromophores, a class of compounds with myriad applications. Here, we show that visible-light photoexcitation of halogenated boron-dipyrromethene (BODIPY) chromophores enables Ni-catalyzed Suzuki–Miyaura cross-coupling reactions under mild conditions (**Figure 1d**). These conditions are selective for the BODIPY substrate in the presence of aryl iodides that do not absorb visible light. Moreover, the substrate photoexcitation mechanism exhibits high chemoselectivity correlated to the photophysics of the substrate.
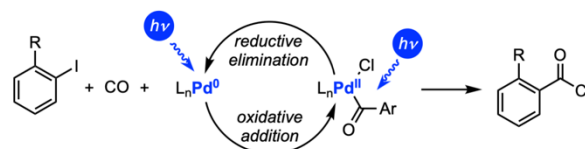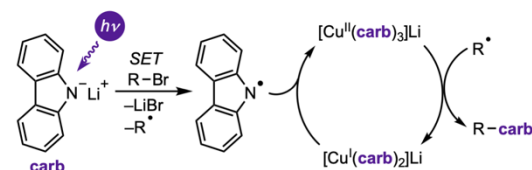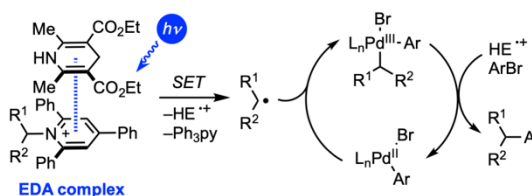

Figure 1. Examples of light driving transition-metal-catalyzed (a) carbonylation, (b) amination, and (c) deaminative cross-coupling in the absence of photoredox catalysts. In this work (d), chromophores can be selectively functionalized through substrate photoexcitation. HE = Hantzsch ester.

Organic chromophores are commonly used as photoredox catalysts because of their low cost and synthetic tunability.[14] In isolated cases, light-absorbing substrates and products have been shown to act as photoredox catalysts to mediate their own functionalization or formation through SET.[15–17] We imagined that the same excited-state properties that make a chromophore an effective photoredox catalyst—high triplet yields, long excited-state lifetimes, and high excited-state redox potentials—could be used to engage a ground-state transition-metal catalyst in a photoinduced cross-coupling. A key advantage of metallophotoredox cross-coupling mechanisms is accessing the reactivity of one-electron chemistry while bypassing unselective free radical intermediates.[18] We hypothesized that photoexcitation of the substrate could induce SET with the transition-metal catalyst to enter a reaction manifold with not just lower barriers, but with distinct *selectivity* compared to thermal cross-coupling conditions. Such a photoinduced cross-coupling reaction could exhibit selectivity in the presence of multiple substrates with similar sterics or electronics but distinct excited-state properties.

In this work, we show that the photoinduced Ni-catalyzed cross-coupling of diiodo-BODIPY chromophores is mild and selective. These conditions are not only selective for the BODIPY substrate in the presence of aryl halides that do not absorb visible light, but are also highly selective for mono *vs.* bis addition. Mono-substituted products may be further elaborated by thermal cross-coupling reactions to yield donor-acceptor BODIPYs. Strikingly, small structural changes at the *meso* position that do not affect the sterics or electrophilicity of the C–I bond result in selective formation of the bis-substituted product. This selectivity is consistent with a substrate photoexcitation mechanism that involves SET to the triplet state. Finally, we show that a mixture of halogenated BODIPYs with similar absorption spectra undergo selective photoinduced cross-coupling, in contrast to a thermal reaction that delivers a complex mixture of products. This result suggests that substrate photoexcitation mechanisms can confer unique selectivity on cross-coupling reactions, potentially enabling the identification of triplet sensitizers and photooxidants from mixtures of halogenated chromophores.

RESULTS AND DISCUSSION

1. Reaction development

We turned our initial focus to halogenated BODIPY chromophores as substrates for the photoinduced cross-coupling reaction. This selection was guided by the broad utility of BODIPY derivatives as photosensitizers and photocatalysts for transformations including oxidations,[19,20] oxidative couplings,[21–23] cross coupling,[24] atom transfer radical addition,[25] and photopolymerization.[26,27] Furthermore, BODIPYs are ubiquitous fluorophores in materials science and bioimaging due to large absorption coefficients, narrow emission profiles, high photoluminescence quantum yields, and good photostability.[28] Derivatives that access the triplet state are additionally useful for photodynamic therapy[29] and triplet-triplet annihilation

upconversion.[30,31] The photophysical and chemical properties of BODIPYs are highly tunable using modifications to the core. Representative examples include red-shifting the absorption and emission to the near-infrared,[32] increasing the Stokes shift,[28] increasing intersystem crossing to the triplet state,[33] shifting the redox potentials,[34] and inducing responses to viscosity[35] and small molecules.[36]

We hypothesized that the identity of the halogen on the BODIPY electrophile would strongly affect cross-coupling reactivity by virtue of its effect on C–X bond strength, redox potential, and photophysics. In cross-coupling reactions, the rate of oxidative addition typically follows the trend I > Br > Cl. Similarly, the identity and quantity of halogens is expected to strongly influence the BODIPY excited state. Halogenated BODIPY chromophores are frequently used as triplet photosensitizers thanks to the internal heavy-atom effect,[37–40] and the same trend (I > Br > Cl) is observed for intersystem crossing efficiency (Φ_{ISC}).[41] If the substrate reacts in its excited state, we also expect to see an effect of the *meso* substituent on BODIPY. This substituent significantly affects the singlet excited-state lifetime and rate of decay by nonradiative internal conversion through the free rotor effect.[35,42]

Therefore, we began our reaction development with diiodo-BODIPY chromophore **1**, a known photosensitizer[37] and photocatalyst[43] that absorbs green light. We found promising reactivity with Ni catalysts, which are commonly employed in metallophotoredox reactions due to their propensity for single-electron chemistry.[44–47] Multiple mechanisms have been proposed for the role of light in these reactions, including oxidation-state modulation by a photoredox catalyst,[48–51] direct photoexcitation of Ni(II) complexes,[52] and recovery of inactive, off-cycle Ni(II) species by photoreduction.[53,54] Under the optimized conditions, **1** underwent Suzuki–Miyaura cross-coupling at room temperature under irradiation with green light in the presence of Ni(dppp)Cl$_2$ precatalyst. Even though excess 4-methoxyphenyl boronic acid (**2**) was used, mono-substituted BODIPY **3a** was selectively formed in 82% yield (**Table 1,** entry 1). No bis-substituted product **3b** could be detected in the crude reaction mixture by LCMS or ^{1}H NMR. This chemoselectivity is notable in comparison to traditional thermal Pd-catalyzed conditions (entry 2), which favor the bis-substituted product **3b**. To confirm the role of light and catalyst for the photoinduced conditions, we performed several control reactions. No product was observed in the absence of Ni catalyst (entry 3), and 10% yield was obtained when the reaction was conducted in the dark (entry 4). Under thermal conditions (78 °C) in the dark, both **3a** and **3b** were observed in low yield and in nearly equal quantities (entry 5), suggesting that the photoinduced reaction achieves selectivity through a distinct mechanism. Intriguingly, substituting Ni(dppp)Cl$_2$ with Pd(OAc)$_2$/dppp under the optimal photoinduced conditions also delivered **3a** as the major product, albeit with lower yield and selectivity, suggesting that the mechanism governing mono-selectivity could be general for different transition-metal catalysts.

Table 1. Optimization for the nickel-catalyzed photoinduced Suzuki–Miyaura reaction
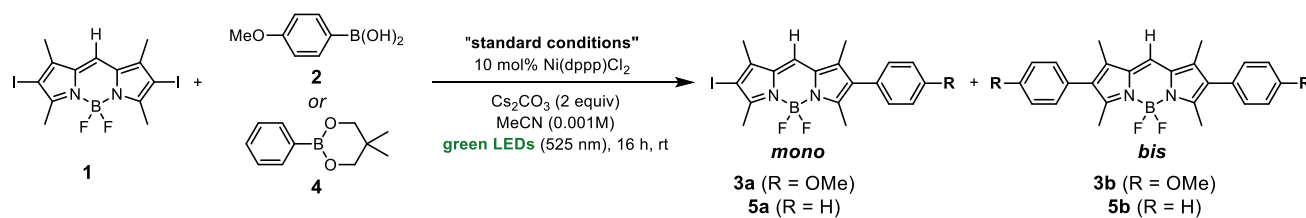
nucleophile	entry	deviation from "standard conditions"[a]	% conversion	% yield[b]	mono:bis
2	1	none (**Condition A**)	100	**82**	**>15:1**
	2	10% Pd(PPh₃)₄, Na₂CO₃, dioxane-H₂O, 100 °C, no light	89	57	1:8
	3	no Ni(dppp)Cl₂	12	<5	-
	4	no light	26	10	>15:1
	5	78 °C, no light	49	14	1:1.3
	6	10 mol% Ni(COD)₂, 12 mol% of (PCy₂)₂ethane, toluene-dioxane (**Condition B**)	97	61	12:1
phenyl boronic acid	7	none (**Condition A**)	36	17	>15:1
4	8	**Condition B**	78	**63**	**>15:1**
	9	no Ni(COD)₂ or no ligand	15 - 20	<5	-
	10	no light	26	11	>15:1

[a]All data represent the average of two experiments. Under the standard conditions, the reaction was performed on a 0.004 mmol scale, with 2 equiv cesium carbonate, 10 equiv of 4-methoxyboronic acid, 0.1 equiv of Ni(dppp)Cl₂, and degassed acetonitrile (0.001 M). Irradiation was provided by green LEDs using fan cooling to maintain a temperature of <30 °C. See SI for details. [b]Conversion, yield, and ratio of mono to bis products were determined by LCMS using Erythrosine-B as external standard.

When we sought to expand the nucleophile scope to electron-neutral boronic acids, disappointingly, the standard conditions (Condition A) delivered low yields of cross-coupled product (entry 7). Therefore, the catalyst, ligand, solvent, and nucleophile were re-evaluated. We found that a combination of Ni(COD)₂ and (PCy₂)₂ethane ligand in a mixed solvent of toluene and dioxane, using the neopentyl glycol ester **4**, yields the desired phenyl-substituted BODIPY chromophore **5a** in 63% yield with high chemoselectivity (entry 8, Condition B). Other bisphosphine ligands such as dppe and dppp also provide good yields (SI, Table S6). We repeated the key control reactions using these modified conditions and again saw no product in the absence of catalyst and 11% yield in the absence of light (entries 9 and 10), consistent with a Ni-catalyzed, light-promoted reaction. Condition B is also applicable to electron-rich boronic acids, albeit with slightly lower yield and chemoselectivity (entry 6).

We hypothesized that green LEDs (centered at 525 nm, FWHM 30 nm; SI, Figures S9-S13) would promote the reaction with the highest efficiency due to the substrate's maximum absorbance at 531 nm. To test this hypothesis, we performed the reaction with LEDs ranging from UV (350 nm) to red (626 nm). As expected, based on the absorption spectrum of **1**, under both Condition A and B, green LEDs yielded the desired product in the highest yield. Identical reactions with UV, violet, and red LEDs resulted in low conversions with no desired product, and blue, yellow, and white[55] LEDs provided low yields of product (**Figure 2**). The sensitivity of this reaction to the color of the light further suggests that a thermal reaction is not responsible for catalysis. Other components of the reaction, such as the boronic acid/ester and the Ni precatalyst, do not absorb green light, also supporting the hypothesis that the BODIPY substrate or derivative thereof is involved in the light-dependent step.
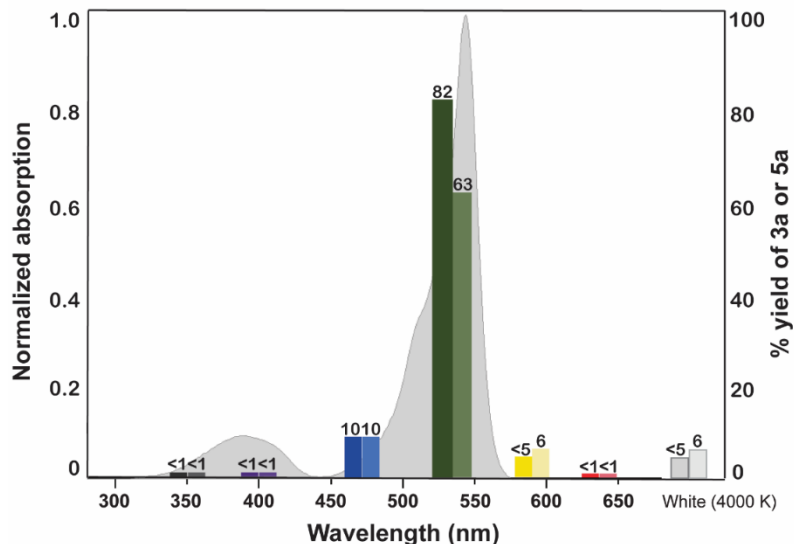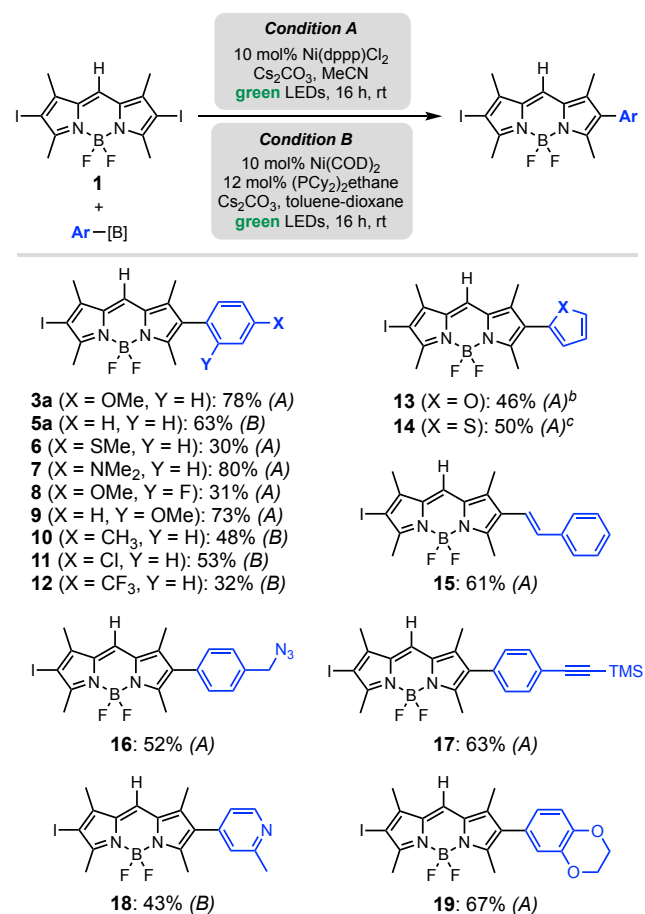
Figure 2. Wavelength screen for the photoinduced nickel-catalyzed Suzuki-Miyaura reaction between BODIPY **1** and boronic acid **2** under Condition A (dark bars), or boronic ester **4** under Condition B (faded bars). The normalized UV-Vis absorption spectrum of BODIPY **1** is superimposed in the background. See SI for details.

2. Substrate scope

Based on our optimization studies in **Table 1**, we next explored the scope of the photoinduced cross-coupling reaction with respect to boronic acid/ester coupling partner. On preparative scale, it was possible to increase the concentration to 0.01 M without sacrificing yield or chemoselectivity (see SI, Table S2 and S5 for details). Using Condition A, electron-rich aromatic, heteroaromatic, and vinyl boronic acids provided the mono-functionalized products in 30–80% isolated yield. Minor bis-substituted products were only observed in the crude reaction mixture when using 5-membered heteroaromatic boronic acids (**13** and **14**, ~6-8:1). Azide- and alkyne-substituted boronic acids furnished BODIPYs **16** and **17** with handles for conjugation by Cu-catalyzed click chemistry. Under Condition B, electron-neutral and -poor boronic esters provided mono-substituted products in 32–63% isolated yield, accompanied by unreacted starting material (8–25%); the modest reactivity of electron-poor nucleophiles remains a limitation of this method (**Table 2**).

Table 2. Nucleophile scope for the photoinduced nickel-catalyzed Suzuki–Miyaura reaction[a]


3a (X = OMe, Y = H): 78% *(A)*
5a (X = H, Y = H): 63% *(B)*
6 (X = SMe, Y = H): 30% *(A)*
7 (X = NMe$_2$, Y = H): 80% *(A)*
8 (X = OMe, Y = F): 31% *(A)*
9 (X = H, Y = OMe): 73% *(A)*
10 (X = CH$_3$, Y = H): 48% *(B)*
11 (X = Cl, Y = H): 53% *(B)*
12 (X = CF$_3$, Y = H): 32% *(B)*

13 (X = O): 46% *(A)[b]*
14 (X = S): 50% *(A)[c]*

15: 61% *(A)*

16: 52% *(A)*

17: 63% *(A)*

18: 43% *(B)*

19: 67% *(A)*

[a] Reactions were performed on a 0.024 mmol scale, with 2 equiv cesium carbonate, 10 equiv boronic acid/ester, and 0.1 equiv Ni(dppp)Cl$_2$ in degassed acetonitrile (0.01 M) for Condition A, or 0.1 equiv Ni(COD)$_2$ and 0.12 equiv (PCy$_2$)$_2$ethane in degassed toluene-dioxane (1:1, 0.01 M) for Condition B, under irradiation by green LEDs

with fan cooling to maintain <30 °C. Products were purified by flash column chromatography. [b] The crude reaction mixture was a 6.7:1 ratio of mono:bis products. [c] The crude reaction mixture was a 8.2:1 ratio of mono:bis products.

The high chemoselectivity of the photoinduced reaction stands in contrast to typical thermal cross-coupling conditions. The selective activation of C–X bonds in polyhalogenated aromatic and heteroaromatic substrates is most often based on intrinsic reactivity differences between sites on the (hetero)aromatic scaffold[56,57] or between C–X bonds (i.e., I > Br > Cl).[58–60] In Pd-catalyzed cross-coupling reactions of polyhalogenated (hetero)aromatics, the identity of the ligand can be used to enhance or even invert the substrate's intrinsic selectivity.[59] For substrates with multiple identical C–X bonds, however, a statistical mixture is often observed, even when equimolar amounts of the nucleophile are used. Monoselectivity can only be achieved if the first substitution deactivates the remaining C–X bonds through steric or electronic effects,[61] or causes a significant change in crystallinity (solvent-free conditions).[62]
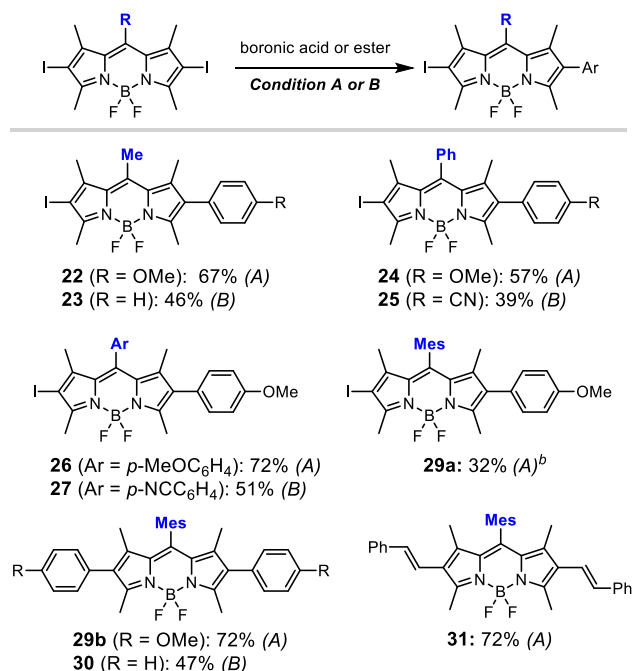
In our light-dependent reaction, the mono-substituted products are deactivated towards the photoinduced cross-coupling, but not to thermal conditions. Thus, the remaining C–I bond can be engaged in thermal cross-coupling reactions to deliver unsymmetrically substituted BODIPY chromophores, which are found in dyads and triads designed for light harvesting, nonlinear optics, and bioconjugation.[33,63–67] To highlight the utility of this strategy, we applied our protocol to the construction of BODIPYs containing electron donors and acceptors at the 2 and 6 positions. The conventional route to prepare such donor-acceptor BODIPYs relies on sequential mono-halogenation, cross-coupling, halogenation, and cross-coupling, rendering this stepwise sequence inefficient (10% overall yield).[68] In contrast, the photoinduced cross-coupling of diiodo-BODIPY 1 with an electron-rich (donor) arylboronic acid selectively delivers the mono-substituted product (3a or 7) in high yield. This intermediate can be directly elaborated with an electron-poor (acceptor) boronic acid using traditional thermal, Pd-catalyzed cross-coupling conditions (**Scheme 1**). This route was used to prepare donor-acceptor BODIPYs 20 and 21 in 40–45% overall yield over 3 steps from the commercial laser dye BODIPY 505/515 (CAS 21658-70-8). Thus, the photoinduced cross-coupling protocol improves synthetic access to unsymmetrically substituted BODIPYs for material applications.

Scheme 1. Synthesis of unsymmetrical BODIPY chromophores by photoinduced cross-coupling.
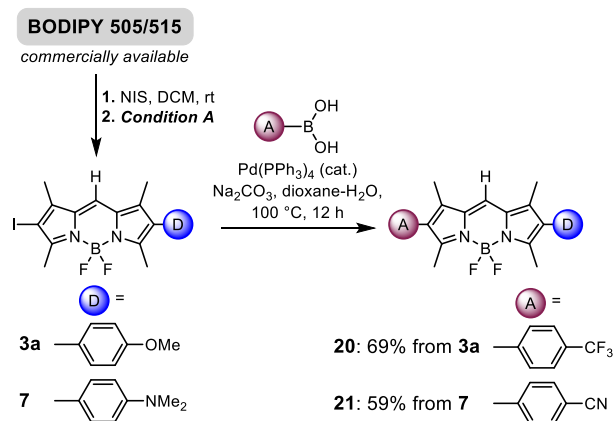
Next, we explored the scope of this cross-coupling with respect to the BODIPY substrate (**Table 3**). Diiodo-BODIPYs containing methyl, phenyl, or *para*-substituted aryl groups at the *meso* position all provided the mono-substituted products in 34–72% yield, using Condition A for electron-rich boronic acids (**22**, **24**, **26**) and Condition B for electron-neutral and -poor boronic esters (**23**, **25**). Surprisingly, placing a sterically hindered mesityl substituent at the *meso* position (BODIPY **28**) altered the chemoselectivity of the photoinduced cross-coupling. Under the standard conditions (16 h), exclusively bis-substituted product **29b** was observed and isolated in 72% yield. By running the reaction to incomplete conversion (5 h), we could obtain a 1:2 ratio of mono- to bis-substituted products and isolate **29a** in 32% yield. These results suggest that mesityl-BODIPY **28** continues to react after the initial mono-substitution, unlike the other chromophores studied. Bis-substitution was also observed for the reaction of **28** with other boronic acids and esters under Conditions A and B (**30, 31**).

Table 3. BODIPY scope for the photoinduced nickel-catalyzed Suzuki–Miyaura reaction[a]

22 (R = OMe): 67% (A)
23 (R = H): 46% (B)

24 (R = OMe): 57% (A)
25 (R = CN): 39% (B)

26 (Ar = p-MeOC₆H₄): 72% (A)
27 (Ar = p-NCC₆H₄): 51% (B)

29a: 32% (A)[b]

29b (R = OMe): 72% (A)
30 (R = H): 47% (B)

31: 72% (A)

[a] Reactions were performed on a 0.024 mmol scale, with 2 equiv cesium carbonate, 10 equiv boronic acid, and 0.1 equiv Ni(dppp)Cl₂ in degassed acetonitrile (0.01 M) for Condition A, or 0.1 equiv Ni(COD)₂ and 0.12 equiv (PCy₂)₂ethane in degassed toluene-dioxane (1:1, 0.01 M) for Condition B, under irradiation by green LEDs with fan cooling to maintain <30 °C. Products were purified by flash column chromatography. [b] The reaction was stopped after 5 h.

Finally, we sought to determine whether chromophores with red-shifted absorption can undergo the photoinduced cross-coupling with even lower-energy light. Aza-BODIPYs are red-shifted relative to BODIPYs due to the electronegative N atom lowering the energy of the LUMO.[69] This effect, in combination with electron-rich aryl substituents, results in chromophores that absorb in the red to near-IR ranges.[70,71] Halogenated aza-BODIPYs have been used as photosensitizers for singlet oxygen generation[72,73] and photoredox catalysts for radical polymerization[26]. We found that aza-BODIPY **32** (λ_{max} = 658 nm) underwent photoinduced Suzuki–Miyaura cross-coupling to deliver mono-substituted product **33** in 28% yield (**Scheme 2**). Future work will include the optimization of photoinduced cross-coupling conditions for these red-shifted substrates.

Scheme 2. Cross-coupling of aza-BODIPY with red light[a]

32 (λ_{max} 658 nm)

33: 28% NMR yield
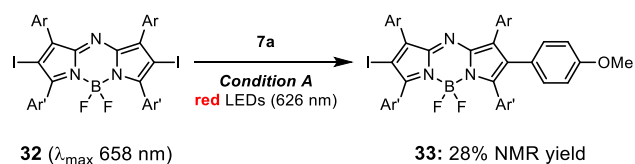
[a] Ar = 3,4,5-trimethoxybenzene; Ar' = 4-tBuPh.

In summary, we have discovered that diiodo-BODIPY and aza-BODIPY chromophores undergo Ni-catalyzed coupling when irradiated with light corresponding to their absorption maxima. However, while all BODIPY substrates evaluated exhibit similar absorption and emission profiles (SI, Figure S18), their reactivity patterns differ significantly. Therefore, to better understand the selectivity of the photoinduced cross-coupling reaction, we probed the nature of the light dependence and the photophysical and photochemical properties of the substrates in greater detail.

3. Photoinitiation vs. photocontrol

Figure 2 shows that the optimal wavelengths of the photoinduced cross-coupling correspond to the absorption of the BODIPY substrate. We sought to establish whether the reaction is photoinitiated or photocontrolled. If the reaction is photoinitiated, product formation should continue in the dark after a period of initial irradiation. We monitored the conversion of **1** under Condition A as a function of time during alternating green irradiation and dark. During the periods with green irradiation, we saw significant conversion of **1** to mono-substituted product **3a**. During the dark periods, we continued to see conversion of **1** but minor formation of **3a** (<5% yield in 5 hours), consistent with the unproductive background decomposition that occurs in the dark (Table 1, entry 4). The difference in the rate of product formation between the irradiated and dark periods suggests that some thermal background reaction can occur in the dark, representing less than one catalyst turnover, but the productive reaction is significantly accelerated (and the decomposition suppressed) under irradiation.
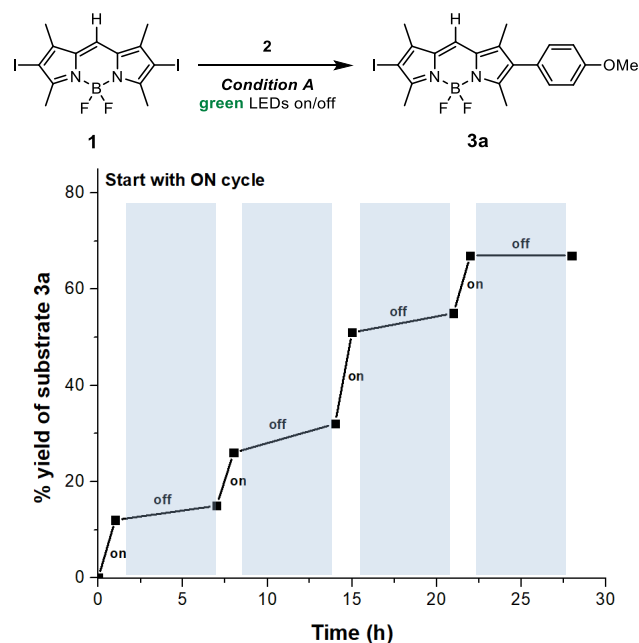
Figure 3. On/off experiment with BODIPY **1** under Condition A. Measurements were taken at an interval of 1 hr for the ON cycle and 6 hrs for OFF cycle. See SI for details.

4. Excited-state properties of the substrates and products

To rationalize the observed reactivity and selectivity under irradiation wavelengths corresponding to substrate absorption, we next turned our attention towards the excited-state properties of the BODIPY substrates. Since the identity and number of halogens is expected to significantly influence excited-state properties,[40] we also
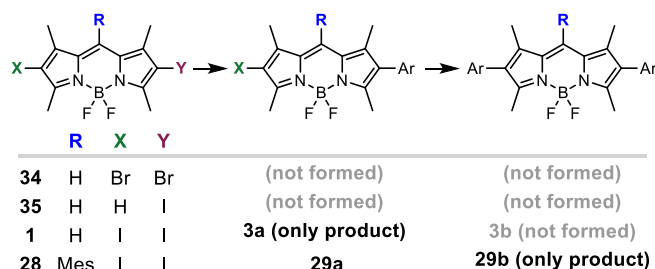
6

prepared dibromo-BODIPY **34** and monoiodo-BODIPY **35**. Under Conditions A and B, neither **34** nor **35** formed any detectable cross-coupled product. While the inertness of **34** could be explained by the lower reactivity of C–Br bonds towards oxidative addition, the absence of reactivity for **35**, which only differs from substrate **1** by one iodine atom, suggests a photophysical or photochemical origin for selectivity.

We compared these unreactive substrates to **1**, its mono-substituted product **3a**, and mesityl-BODIPY **28**, which forms bis-substituted **29b** via intermediate **29a**. We reasoned that the conversion of **1** to **3a** must be accompanied by a significant change in its photophysical or photochemical properties, which prevent further cross-coupling to form **3b**. We also anticipated that **3a** might

have similar properties to **35**, which was also unreactive despite absorbing green light. In contrast, we expected that **28** and **29a** should possess similar excited-state properties, explaining why the reaction continues after the first cross-coupling to form **29b**.

For these compounds, we measured the ground-state absorption spectra, steady-state fluorescence spectra, fluorescence lifetimes (τ_S), fluorescence quantum yields (Φ_{FL}), and intersystem crossing quantum yields (Φ_{ISC}). The collection of these data permitted the calculation of the radiative decay rate constant (k_r), the non-radiative decay rate constant (k_{nr}), and the intersystem crossing rate constant (k_{ISC}). The photochemical and photophysical data are summarized in **Table 4**; additional data are shown in Table S9 and representative datasets are illustrated in Figures S17-S23 (SI).

Table 4. Excited-state properties of BODIPY chromophores

compound	λ_{abs}[a]	λ_{em}[a]	τ_S (ns)[b]	τ_T (μs)[c]	Φ_F[d]	Φ_Δ[e]	k_r (10^8 s^{-1})	k_{nr} (10^8 s^{-1})	k_{isc} (10^8 s^{-1})	E_{red} (V)[f]	E_T (eV)[g]	$E_{red,T}$ (V)[h]
34	538	551	1.70	n.d.	0.22	0.67	1.30	0.65	3.94	-1.29	1.59	0.30
35	525	539	0.23	1.8	0.03	0.84	1.30	5.65	36.5	-1.43	1.57	0.14
1	532	553	0.31	2.1	0.02	0.94	0.65	3.23	28.4	-1.30	1.55	0.25
3a	530	601	0.62	3.1	0.05	0.45	0.82	8.20	7.38	-1.40	1.58	0.18
28	531	548	0.29	0.85, 53.4%	0.02	0.87	0.67	4.33	28.3	-1.35	1.64	0.29
29a	528	585	0.67	6.7	0.06	0.62	0.90	4.78	9.25	-1.40	1.63	0.23

[a]Unit = nm, concentration = 1.0 x 10^{-5} M in acetonitrile. [b]τ_S = Fluorescence lifetime in nanoseconds, measured by time-resolved photoluminescence (concentration = 1.0 x 10^{-6} M in acetonitrile). Fluorescence lifetime data were fit to a mono-exponential decay. [c]τ_T = Triplet lifetime in microseconds, measured by microsecond transient absorption in toluene (concentration = 1.0 x 10^{-6} M in acetonitrile). [d]Φ_F = Absolute fluorescence quantum yields determined by integrating sphere (concentration = 1.0 X 10^{-6} M in acetonitrile). [e] Φ_Δ = Phosphorescence quantum yield of singlet oxygen ($^1O_2$) phosphorescence with phenazine as standard. [g]Onset potentials shown in V. All electrochemical measurements were performed in acetonitrile (0.1 M n-Bu$_4$NPF$_6$) using Ag/AgCl wire as a pseudo-reference electrode and referenced to ferrocene/ferrocenium redox couple. [h]Triplet energies were determined by λ_{max} of the phosphorescence spectrum at 77K in 2:2:1:1 (v:v) ethyl iodide/diethyl ether/ethanol/toluene. See SI for spectra. [h]Approximated as $E_{red,T} = E_T + E_{red}$.

The normalized ground-state absorption and steady-state fluorescence spectra of chromophores **34, 35, 1, 3a, 28** and **29a** were collected in acetonitrile, representative of Condition A (SI, Figure S17). The absorption spectra of all six derivatives are similar, exhibiting maxima between 525 and 538 nm and narrow absorption transitions with high extinction coefficients and vibronic progression characteristic of π-π* transitions. The similarities suggest that differences in the absorption are not responsible for the changes in reactivity. The fluorescence spectra of all chromophores are also assigned as π-π* in nature, but the mono-substituted products **3a** and **29a** exhibit larger Stokes shifts and broader emission than the initial substrates, suggesting charge-transfer character in their singlet π-π* excited states.

The singlet excited-state dynamics in these molecules are influenced by their halogen content, arylation at the 6-position, and the nature of the substituent in the *meso* position. The dibromo-BODIPY **34** exhibits the highest fluorescence quantum yield (0.22). All of the iodinated chromophores possess low fluorescence quantum yields (0.02–0.11) and fluorescence lifetimes under a nanosecond, suggesting that the singlet excited state is too short-lived to undergo bimolecular reactions. Therefore, intersystem crossing (ISC) to a long-lived triplet state is likely responsible for the observed reactivity. ISC is the dominant kinetic pathway in both of the diiodo-BODIPY derivatives (**1** and **28**) and mono-iodo-BODIPY **35**. These compounds have similar ISC crossing rate

constants on the order of $3 \times 10^9 \, s^{-1}$, resulting in quantum yields for ISC exceeding 0.8.

Coupling installs an aryl group that increases possible non-radiative decay pathways by vibration, rotation, and intramolecular charge transfer.[74–76] Correspondingly, the mono-functionalized derivatives **3a** and **29a** exhibit higher rates of both radiative and nonradiative decay, compared to their diiodo-BODIPY precursors. However, the *meso* substituents have an impact on the relative magnitude of the changes that occur after cross-coupling. Both **3a** and **29a** experience a decrease in ISC rate and quantum yield compared to their precursors. In **3a**, the rate of nonradiative decay $(8.2 \times 10^8 \, s^{-1})$ becomes competitive with ISC $(7.4 \times 10^8 \, s^{-1})$; in contrast, for **29a**, ISC remains twice as fast compared to nonradiative decay $(9.2 \times 10^8 \, s^{-1}$ vs. $4.7 \times 10^8 \, s^{-1})$. Compared to smaller substituents, the mesityl group is particularly effective at decreasing internal conversion by limiting the free rotor effect.[42,77] Nevertheless, these differences in ISC cannot fully explain the difference in reactivity between **3a** and **29a** because mono-iodo-BODIPY **35** exhibits high quantum yield and rate for ISC, but does not undergo cross-coupling. Furthermore, all of the iodinated BODIPYs measured had triplet lifetimes 0.85 μs or greater, and we did not observe any trend between triplet lifetime and reactivity. These data suggest that formation of a triplet state is a necessary precondition to reactivity but not the basis for mono vs. bis chemoselectivity.

Since iodo-BODIPYs are competent photoredox catalysts,[43] we next evaluated the photochemical reactivity of the triplet states. The ground-state redox potentials were determined by cyclic voltammetry (SI, Figures S1-S7 and S14-S15), and the triplet energies (E_T) were determined by phosphorescence measurements in a solvent glass at 77 K (SI, Figures S23). The excited-state oxidation potentials fell between –0.68 and –0.82 vs. Fc/Fc$^+$ (SI, Table S9) and did not reveal any trends consistent with the reactivity: that is, unreactive product **3a** has a similar excited-state oxidation potential to reactive intermediate **29a** (–0.80 and –0.82 V), and unreactive substrate **35** (–0.73 V) is a better excited-state reductant than substrate **1** (–0.68 V). However, the excited-state reduction potentials reveal a clear cutoff between reactive substrates (**1, 28, 29a** ≥0.23 V) and unreactive substrates (**35, 3a** ≤0.18 V). This 70 mV difference in excited-state reduction potentials corresponds to a 1.61 kcal/mol difference in thermodynamic driving force for electron transfer.

Taken together, we find that the photoinduced cross-coupling reaction is exquisitely sensitive to the excited-state properties of the substrate. The reaction is capable of distinguishing between substrates with similar absorption, sterics, and electronics, based on subtly different excited-state reduction potentials. The observed trends are consistent with the substrate triplet state acting as a photooxidant for oxidative addition by SET[45] or oxidation-state modulation of a Ni intermediate[48–51] or off-cycle species.[54] However, our data do not rule out scenarios that involve photoexcitation of Ni-BODIPY complexes.[52]

Three representative scenarios in which photoexcitation of the substrate or a Ni complex derived from it promote the cross-coupling cycle are presented in **Figure 4**. In scenario (a), an example of oxidation-state modulation, ^{3}BODIPY oxidizes an on-cycle Ni(II) intermediate, forming a Ni(III) intermediate that undergoes facile reductive elimination. In scenario (b), ^{3}BODIPY undergoes SET with Ni(0) to form an ion pair, which undergoes collapse to the oxidative addition product in a photoinduced variation of the classic mechanism elucidated by Kochi.[45] Alternatively, in scenario (c),

photoexcitation of a Ni(II)–BODIPY adduct is required for catalytic turnover.
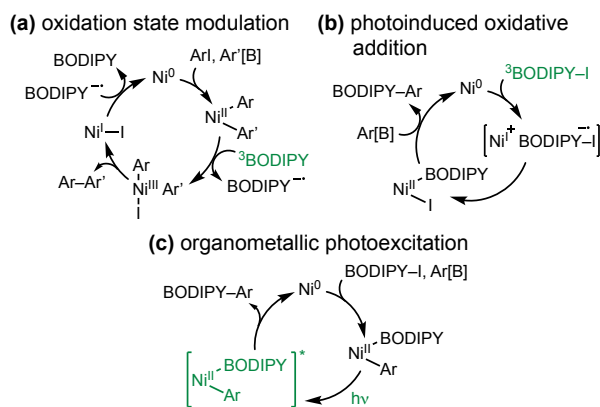

Figure 4. Representative possible mechanisms that involve photoexcitation of BODIPY or an organometallic intermediate. For simplicity, inorganic byproducts are not included.

5. Selectivity of the photoinduced reaction with mixtures of substrates

If scenario (a) is operative, the substrate that undergoes cross-coupling need not be photoactive. In that scenario, the BODIPY substrate can be viewed as a photoredox catalyst that should, in principle, be able to promote the cross-coupling of other ground-state substrates in concert with Ni catalysis. To test this hypothesis, we performed competition experiments between **1** and substrates that do not undergo photoinduced cross-coupling. First, we examined the chemoselectivity of the photoinduced cross-coupling in the presence of a simple aryl halide, 2-fluoroiodobenzene (**36**), which does not absorb past 300 nm (SI, Figure S24). While **36** undergoes efficient Suzuki–Miyaura cross-coupling under thermal conditions with various Pd catalysts,[78] in a competition experiment between **1** and **36** (1:10 molar ratio) under Condition A, we observed exclusive formation of **3a** arising from mono-arylation of **1** (**Scheme 3**). By ^{19}F NMR, we observed neither conversion of **36** nor formation of the expected biphenyl product (SI, Figure S25).

Scheme 3. Competition experiment between BODIPY 1 and 4-fluoroiodobenzene
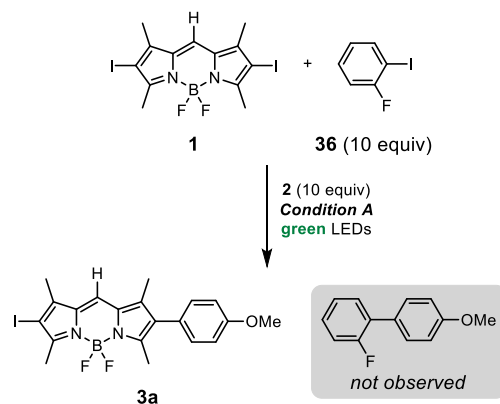

Next, we sought to test the chemoselectivity of this reaction in the presence of multiple substrates with similar absorption but different excited-state properties. A 1:1:1 mixture of **1, 34,** and **35** was subjected to Condition A with excess arylboronic acid (**Scheme 4**). Again, only the monosubstituted product **3a** derived from **1** could be observed by ^{1}H NMR and high-resolution mass spectrometry; **34** and **35** were recovered unreacted (SI, Figures S26-29). Under

standard thermal Pd-catalyzed conditions, a complex mixture of products arising from **1**, **34**, and **35** is observed (SI, Figure S30).

Scheme 4. Competition experiment between BODIPYs[a]

34 + **35** + **1**

2 (10 equiv)
Condition A
green LEDs

3a (sole product)
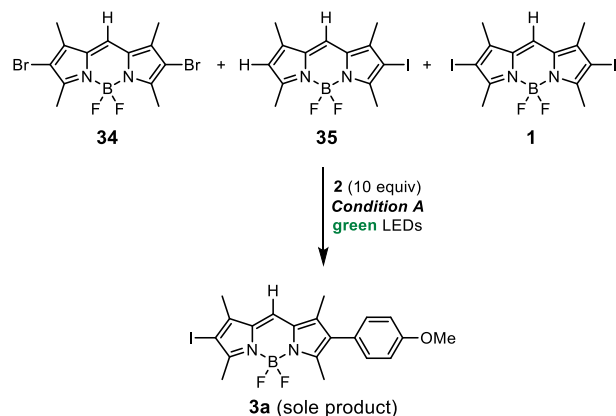
[a]Reactions were performed on a 0.004 mmol scale, with 1:1:1 ratio of **1**, **34**, and **35**, 2 equiv Cs_2CO_3, 10 equiv boronic acid, and 0.1 equiv $Ni(dppp)Cl_2$ in degassed acetonitrile (0.001 M) under irradiation by green LEDs with fan cooling to maintain <30 °C. Conversion, yield, and ratio of starting materials to products were determined by ^{1}H-NMR using dibromomethane as external standard.

Therefore, we can rule out mechanistic scenarios in which the BODIPY chromophore acts as a photoredox catalyst or photosensitizer[79] to activate on- or off-cycle intermediates towards cross coupling (for example, **Figure 4a**). At this stage, we cannot distinguish between mechanisms in which photoexcited BODIPY substrates enter the catalytic cycle (**Figure 4b**) and mechanisms in which an organometallic intermediate containing BODIPY is photoexcited (**Figure 4c**). The isolation and characterization relevant organometallic intermediates to explore this latter possibility are ongoing. Beyond providing insight into the role of substrate photoexcitation in the reaction mechanism, these competition experiments demonstrate that chemoselectivity for the substrate with most efficient ISC and highest excited-state reduction potential is maintained in mixtures of chromophores with similar absorption characteristics.

CONCLUSIONS

We have developed a photoinduced, Ni-catalyzed Suzuki–Miyaura cross-coupling of halogenated BODIPY chromophores. This reaction exhibits high chemoselectivity depending on the identity of the *meso* substituent. For diiodo-BODIPY substrates with small groups at the *meso* position, high chemoselectivity is observed for the mono-functionalized product, providing rapid synthetic access to unsymmetrically substituted BODIPYs. Preliminary results demonstrate that this reactivity can be extended to bathochromically-shifted chromophores such as aza-BODIPYs using red light. Substitution at the *meso* position of diiodo-BODIPY with a mesityl group does not perturb the C–I bonds sterically or electronically, but shifts the reactivity to selective bis-substitution. Comparison of the excited-state properties of reactive and unreactive substrates reveals a cutoff in the excited-state reduction potential that is correlated to reactivity.

We propose that the cross-coupling mechanism involves photoexcitation of the chromophore substrate or an organometallic intermediate derived from it because the optimal wavelengths for reactivity correspond to the substrate absorption. Based on competition experiments, we can rule out scenarios in which the

substrate acts as a photoredox catalyst or photosensitizer. In addition to applications to chromophore synthesis, we envision that the photoinduced cross-coupling will enable the discovery of new triplet sensitizers and photoredox catalysts from complex mixtures of chromophores. Such a goal will require us to broaden the scope of this reaction to classes beyond BODIPY and aza-BODIPY. Efforts to realize this reactivity-driven approach to materials discovery and detailed mechanistic investigations of the organometallic mechanism are underway in our lab.

AUTHOR INFORMATION

Corresponding Authors

Julia A. Kalow – Department of Chemistry, Northwestern University, Evanston, Illinois 60208, United States.
ORCID ID - orcid.org/0000-0002-4449-9566
Email: jkalow@northwestern.edu

Authors

Pradipta Das – Department of Chemistry, Northwestern University, Evanston, Illinois 60208, United States.
ORCID ID - orcid.org/0000-0002-6530-8909

Eliot F. Woods – Department of Chemistry, Northwestern University, Evanston, Illinois 60208, United States.
ORCID ID - orcid.org/0000-0003-3912-1195

Jack T. Ly – Air Force Research Laboratory, Materials and Manufacturing Directorate, Wright-Patterson Air Force Base, Dayton, Ohio 45433, United States.
UES Inc., Dayton, Ohio 45432, United States.
ORCID ID - orcid.org/0000-0001-9164-508X

Jack N. Olding – Applied Physics Graduate Program, Northwestern University, Evanston, Illinois 60208, United States.
ORCID ID - orcid.org/0000-0001-6907-5316

Kayla F. Presley – Air Force Research Laboratory, Materials and Manufacturing Directorate, Wright-Patterson Air Force Base, Dayton, Ohio 45433, United States.
UES Inc., Dayton, Ohio 45432, United States.
ORCID ID - orcid.org/0000-0001-9091-3214

Brennan Romanoff – Department of Physics, United States Air Force Academy, Colorado 80840, United States

Tod A. Grusenmeyer – Air Force Research Laboratory, Materials and Manufacturing Directorate, Wright-Patterson Air Force Base, Dayton, Ohio 45433, United States
ORCID ID - orcid.org/0000-0002-1842-056X

Emily A. Weiss – Department of Chemistry, Northwestern University, Evanston, Illinois 60208, United States.
Department of Material Science and Engineering, Northwestern University, Evanston, Illinois 60208, United States.
Applied Physics Graduate Program, Northwestern University, Evanston, Illinois 60208, United States.
ORCID ID - orcid.org/0000-0001-5834-463X

REFERENCES

(1) Twilton, J.; Le, C.; Zhang, P.; Shaw, M. H.; Evans, R. W.; MacMillan, D. W. C. The Merger of Transition Metal and Photocatalysis. *Nat. Rev. Chem.* **2017**, *1*, 1 – 17.

(2) Bissember, A. C.; Lundgren, R. J.; Creutz, S. E.; Peters, J. C.; Fu, G. C. Transition-Metal-Catalyzed Alkylations of Amines with Alkyl Halides: Photoinduced, Copper-Catalyzed Couplings of Carbazoles. *Angew. Chem. Int. Ed.* **2013**, *52*, 5129 – 5133.

(3) Kainz, Q. M.; Matier, C. D.; Bartoszewicz, A.; Zultanski, S. L.; Peters, J. C.; Fu, G. C. Asymmetric Copper-Catalyzed C-N Cross-Couplings Induced by Visible Light. *Science* **2016**, *351*, 681 – 684.

(4) Ahn, J. M.; Ratani, T. S.; Hannoun, K. I; Fu, G. C.; Peters, J. C. Photoinduced, Copper-Catalyzed Alkylation of Amines: A Mechanistic Study of the Cross-Coupling of Carbazole with Alkyl Bromides. *J. Am. Chem. Soc.* **2017**, *139*, 12716 – 12723.

(5) Parasram, M.; Gevorgyan, V. Visible Light-Induced Transition Metal-Catalyzed Transformations: Beyond Conventional Photosensitizers. *Chem. Soc. Rev.* **2017**, *46*, 6227 – 6240.

(6) Chuentragool, P.; Kurandina, D.; Gevorgyan, V. Catalysis with Palladium Complexes Photoexcited by Visible Light. *Angew. Chem. Int. Ed.* **2019**, *58* (34), 11586 – 11598.

(7) Crisenza, G. E. M.; Faraone, A.; Gandolfo, E.; Mazzarella, D.; Melchiorre, P. Catalytic Asymmetric C–C Cross-Couplings Enabled by Photoexcitation. *Nat. Chem.* **2021**, *13*, 575 – 580.

(8) Torres, G. M.; Liu, Y.; Arndtsen, B. A. A Dual Light-Driven Palladium Catalyst: Breaking the Barriers in Carbonylation Reactions. *Science* **2020**, *368*, 318 – 323.

(9) Dewanji, A.; Bülow, R. F.; Rueping, M. Photoredox/Nickel Dual-Catalyzed Reductive Cross Coupling of Aryl Halides Using an Organic Reducing Agent. *Org. Lett.* **2020**, *22*, 1611 – 1617.

(10) Cybularczyk-Cecotka, M.; Szczepanik, J.; Giedyk, M. Photocatalytic Strategies for the Activation of Organic Chlorides. *Nat. Catal.* **2020**, *3*, 872 – 886.

(11) Fu, Y.; Huang, J.; Wu, Y.; Liu, X.; Zhong, F.; Wang, J. Biocatalytic Cross-Coupling of Aryl Halides with a Genetically Engineered Photosensitizer Artificial Dehalogenase. *J. Am. Chem. Soc.* **2021**, *143*, 617 – 622.

(12) Polites, V. C.; Badir, S. O.; Keess, S.; Jolit, A.; Molander, G. A. Nickel-Catalyzed Decarboxylative Cross-Coupling of Bicyclo[1.1.1]Pentyl Radicals Enabled by Electron Donor–Acceptor Complex Photoactivation. *Org. Lett.* **2021**, *23*, 4828 – 4833.

(13) Yang, T.; Wei, Y.; Koh, M. J. Photoinduced Nickel-Catalyzed Deaminative Cross-Electrophile Coupling for $C(sp^2)$–$C(sp^3)$ and $C(sp^3)$–$C(sp^3)$ Bond Formation. *ACS Catal.* **2021**, *11*, 6519 – 6525.

(14) Romero, N. A.; Nicewicz, D. A. Organic Photoredox Catalysis. *Chem. Rev.* **2016**, *116*, 10075 – 10166.

(15) Sahoo, B.; Hopkinson, M. N.; Glorius, F. External-Photocatalyst-Free Visible-Light-Mediated Synthesis of Indolizines. *Angew. Chem. Int. Ed.* **2015**, *54*, 15545 – 15549.

(16) Wang, D.; Cheng, C.; Wu, Q.; Wang, J.; Kang, Z.; Guo, X.; Wu, H.; Hao, E.; Jiao, L. Visible-Light Excitation of BODIPYs Enables Self-Promoted Radical Arylation at Their 3,5-Positions with Diazonium Salts. *Org. Lett.* **2019**, *21*, 5121 – 5125.

(17) Wang, D.; Guo, X.; Wu, H.; Wu, Q.; Wang, H.; Zhang, X.; Hao, E.; Jiao, L. Visible Light Excitation of BODIPYs Enables Dehydrogenative Enamination at Their α-Positions with Aliphatic Amines. *J. Org. Chem.* **2020**, *85*, 8360 – 8370.

(18) Kancherla, R.; Muralirajan, K.; Sagadevan, A.; Rueping, M. Visible Light-Induced Excited-State Transition-Metal Catalysis. *Trends Chem.* **2019**, *1*, 510 – 523.

(19) Zhang, C.; Zhao, J.; Wu, S.; Wang, Z.; Wu, W.; Ma, J.; Guo, S.; Huang, L. Intramolecular RET Enhanced Visible Light-Absorbing Bodipy Organic Triplet Photosensitizers and Application in Photooxidation and Triplet–Triplet Annihilation Upconversion. *J. Am. Chem. Soc.* **2013**, *135*, 10566 – 10578.

(20) Li, W.; Xie, Z.; Jing, X. BODIPY Photocatalyzed Oxidation of Thioanisole under Visible Light. *Catal. Commun.* **2011**, *16*, 94 – 97.

(21) Huang, L.; Zhao, J.; Guo, S.; Zhang, C.; Ma, J. Bodipy Derivatives as Organic Triplet Photosensitizers for Aerobic Photoorganocatalytic Oxidative Coupling of Amines and Photooxidation of Dihydroxylnaphthalenes. *J. Org. Chem.* **2013**, *78*, 5627 – 5637.

(22) Wang, X.-F.; Yu, S.-S.; Wang, C.; Xue, D.; Xiao, J. BODIPY Catalyzed Amide Synthesis Promoted by BHT and Air under Visible Light. *Org. Biomol. Chem.* **2016**, *14*, 7028 – 7037.

(23) Wang, X.-Z.; Meng, Q.-Y.; Zhong, J.-J.; Gao, X.-W.; Lei, T.; Zhao, L.-M.; Li, Z.-J.; Chen, B.; Tung, C.-H.; Wu, L.-Z. The Singlet Excited State of BODIPY Promoted Aerobic Cross-Dehydrogenative-Coupling Reactions under Visible Light. *Chem. Commun.* **2015**, *51*, 11256 – 11259.

(24) Yang, L.; Huang, Z.; Li, G.; Zhang, W.; Cao, R.; Wang, C.; Xiao, J.; Xue, D. Synthesis of Phenols: Organophotoredox/Nickel Dual Catalytic Hydroxylation of Aryl Halides with Water. *Angew. Chem. Int. Ed.* **2018**, *57*, 1968 – 1972.

(25) Magagnano, G.; Gualandi, A.; Marchini, M.; Mengozzi, L.; Ceroni, P.; Cozzi, P. G. Photocatalytic ATRA Reaction Promoted by Iodo-Bodipy and Sodium Ascorbate. *Chem. Commun.* **2017**, *53*, 1591 – 1594.

(26) Stafford, A.; Ahn, D.; Raulerson, E. K.; Chung, K.-Y.; Sun, K.; Cadena, D. M.; Forrister, E. M.; Yost, S. R.; Roberts, S. T.; Page, Z. A. Catalyst Halogenation Enables Rapid and Efficient Polymerizations with Visible to Far-Red Light. *J. Am. Chem. Soc.* **2020**, *142*, 14733 – 14742.

(27) Lu, P.; Chung, K.-Y.; Stafford, A.; Kiker, M.; Kafle, K.; Page, Z. A. Boron Dipyrromethene (BODIPY) in Polymer Chemistry. *Polym. Chem.* **2021**, *12*, 327 – 348.

(28) Loudet, A.; Burgess, K. BODIPY Dyes and Their Derivatives: Syntheses and Spectroscopic Properties. *Chem. Rev.* **2007**, *107*, 4891 – 4932.

(29) Kamkaew, A.; Lim, S. H.; Lee, H. B.; Kiew, L. V.; Chung, L. Y.; Burgess, K. BODIPY Dyes in Photodynamic Therapy. *Chem Soc Rev* **2013**, *42*, 77 – 88.

(30) Zhao, J.; Xu, K.; Yang, W.; Wang, Z.; Zhong, F. The Triplet Excited State of Bodipy: Formation, Modulation and Application. *Chem. Soc. Rev.* **2015**, *44*, 8904 – 8939.

(31) Chen, K.; Dong, Y.; Zhao, X.; Imran, M.; Tang, G.; Zhao, J.; Liu, Q. Bodipy Derivatives as Triplet Photosensitizers and the Related Intersystem Crossing Mechanisms. *Front. Chem.* **2019**, *7*, 821.

(32) Lu, H.; Mack, J.; Yang, Y.; Shen, Z. Structural Modification Strategies for the Rational Design of Red/NIR Region BODIPYs. *Chem Soc Rev* **2014**, *43*, 4778 – 4823.

(33) Wu, W.; Guo, H.; Wu, W.; Ji, S.; Zhao, J. Organic Triplet Sensitizer Library Derived from a Single Chromophore (BODIPY) with Long-Lived

Triplet Excited State for Triplet–Triplet Annihilation Based Upconversion. *J. Org. Chem.* **2011**, *76*, 7056 – 7064.

(34) Thompson, B. L.; Heiden, Z. *Redox Chemistry of BODIPY Dyes* in *BODIPY Dyes - A Privilege Molecular Scaffold with Tunable Properties*; 2019.

(35) Miao, W.; Yu, C.; Hao, E.; Jiao, L. Functionalized BODIPYs as Fluorescent Molecular Rotors for Viscosity Detection. *Front. Chem.* **2019**, *7*, 825.

(36) Kowada, T.; Maeda, H.; Kikuchi, K. BODIPY-Based Probes for the Fluorescence Imaging of Biomolecules in Living Cells. *Chem. Soc. Rev.* **2015**, *44*, 4953 – 4972.

(37) Yogo, T.; Urano, Y.; Ishitsuka, Y.; Maniwa, F.; Nagano, T. Highly Efficient and Photostable Photosensitizer Based on BODIPY Chromophore. *J. Am. Chem. Soc.* **2005**, *127*, 12162 – 12163.

(38) Yuster, P.; Weissman, S. I. Effects of Perturbations on Phosphorescence: Luminescence of Metal Organic Complexes. *J. Chem. Phys.* **1949**, *17*, 1182 – 1188.

(39) McClure, D. S. Triplet-Singlet Transitions in Organic Molecules. Lifetime Measurements of the Triplet State. *J. Chem. Phys.* **1949**, *17*, 905 – 913.

(40) Ly, J. T.; Presley, K. F.; Cooper, T. M.; Baldwin, L. A.; Dalton, M. J.; Grusenmeyer, T. A. Impact of Iodine Loading and Substitution Position on Intersystem Crossing Efficiency in a Series of Ten Methylated- *Meso* - Phenyl-BODIPY Dyes. *Phys. Chem. Chem. Phys.* **2021**, *23*, 12033 – 12044.

(41) Rey, Y. P.; Abradelo, D. G.; Santschi, N.; Strasser, C. A.; Gilmour, R. Quantitative Profiling of the Heavy-Atom Effect in BODIPY Dyes: Correlating Initial Rates, Atomic Numbers, and $^1O_2$ Quantum Yields: Quantitative Profiling of the Heavy-Atom Effect in BODIPY Dyes: Correlating Initial Rates, Atomic Numbers, and $^1O_2$ Quantum Yields. *Eur. J. Org. Chem.* **2017**, *2017*, 2170 – 2178.

(42) Kee, H. L.; Kirmaier, C.; Yu, L.; Thamyongkit, P.; Youngblood, W. J.; Calder, M. E.; Ramos, L.; Noll, B. C.; Bocian, D. F.; Scheidt, W. R.; Birge, R. R.; Lindsey, J. S.; Holten, D. Structural Control of the Photodynamics of Boron−Dipyrrin Complexes. *J. Phys. Chem. B* **2005**, *109*, 20433 – 20443.

(43) Li, W.; Li, L.; Xiao, H.; Qi, R.; Huang, Y.; Xie, Z.; Jing, X.; Zhang, H. Iodo-BODIPY: A Visible-Light-Driven, Highly Efficient and Photostable Metal-Free Organic Photocatalyst. *RSC Adv.* **2013**, *3*, 13417 – 13421.

(44) Tsou, T. T.; Kochi, J. K. Reductive Coupling of Organometals Induced by Oxidation. Detection of Metastable Paramagnetic Intermediates. *J. Am. Chem. Soc.* **1978**, *100*, 1634 – 1635.

(45) Tsou, T. T.; Kochi, J. K. Mechanism of Oxidative Addition. Reaction of Nickel(0) Complexes with Aromatic Halides. *J. Am. Chem. Soc.* **1979**, *101*, 6319 – 6332.

(46) Tsou, T. T.; Kochi, J. K. Mechanism of Biaryl Synthesis with Nickel Complexes. *J. Am. Chem. Soc.* **1979**, *101*, 7547 – 7560.

(47) Diccianni, J. B.; Diao, T. Mechanisms of Nickel-Catalyzed Cross-Coupling Reactions. *Trends Chem.* **2019**, *1*, 830 – 844.

(48) Ren, H.; Li, G.-F.; Zhu, B.; Lv, X.-D.; Yao, L.-S.; Wang, X.-L.; Su, Z.-M.; Guan, W. How Does Iridium(III) Photocatalyst Regulate Nickel(II) Catalyst in Metallaphotoredox-Catalyzed C–S Cross-Coupling? Theoretical and Experimental Insights. *ACS Catal.* **2019**, *9*, 3858–3865.

(49) Corcoran, E. B.; Pirnot, M. T.; Lin, S.; Dreher, S. D.; DiRocco, D. A.; Davies, I. W.; Buchwald, S. L.; MacMillan, D. W. C. Aryl Amination Using Ligand-Free Ni(II) Salts and Photoredox Catalysis. *Science* **2016**, *353*, 279 – 283.

(50) Terrett, J. A.; Cuthbertson, J. D.; Shurtleff, V. W.; MacMillan, D. W. C. Switching on Elusive Organometallic Mechanisms with Photoredox Catalysis. *Nature* **2015**, *524*, 330 – 334.

(51) Zhu, B.; Yan, L.-K.; Geng, Y.; Ren, H.; Guan, W.; Su, Z.-M. Ir ^{III}/Ni ^{II} -Metallaphotoredox Catalysis: The Oxidation State Modulation Mechanism *versus* the Radical Mechanism. *Chem. Commun.* **2018**, *54*, 5968 – 5971.

(52) Shields, B. J.; Kudisch, B.; Scholes, G. D.; Doyle, A. G. Long-Lived Charge-Transfer States of Nickel(II) Aryl Halide Complexes Facilitate Bimolecular Photoinduced Electron Transfer. *J. Am. Chem. Soc.* **2018**, *140*, 3035 – 3039.

(53) Sun, R.; Qin, Y.; Nocera, D. G. General Paradigm in Photoredox Nickel-Catalyzed Cross-Coupling Allows for Light-Free Access to Reactivity. *Angew. Chem. Int. Ed.* **2020**, *59*, 9527 – 9533.

(54) Sun, R.; Qin, Y.; Ruccolo, S.; Schnedermann, C.; Costentin, C.; Nocera, D. G. Elucidation of a Redox-Mediated Reaction Cycle for Nickel-Catalyzed Cross Coupling. *J. Am. Chem. Soc.* **2019**, *141*, 89 – 93.

(55) 4000K white LEDs, composed of a blue LED and yellow/red phosphors, have significantly less intensity at 525 nm then the green 525nm LEDs. See Figure S13 for emission profile.

(56) Almond-Thynne, J.; Blakemore, D. C.; Pryde, D. C.; Spivey, A. C. Site-Selective Suzuki–Miyaura Coupling of Heteroaryl Halides – Understanding the Trends for Pharmaceutically Important Classes. *Chem. Sci.* **2017**, *8*, 40 – 62.

(57) Legault, C. Y.; Garcia, Y.; Merlic, C. A.; Houk, K. N. Origin of Regioselectivity in Palladium-Catalyzed Cross-Coupling Reactions of Polyhalogenated Heterocycles. *J. Am. Chem. Soc.* **2007**, *129*, 12664 – 12665.

(58) Marshall, J. L.; O'Neal, N. J.; Zakharov, L. N.; Haley, M. M. Synthesis and Characterization of Two Unsymmetrical Indenofluorene Analogues: Benzo[5,6]- *s* -Indaceno[1,2-*b*]Thiophene and Benzo[5,6]-*s*-Indaceno[2,1-*b*]Thiophene. *J. Org. Chem.* **2016**, *81*, 3674 – 3680.

(59) Dobrounig, P.; Trobe, M.; Breinbauer, R. Sequential and Iterative Pd-Catalyzed Cross-Coupling Reactions in Organic Synthesis. *Monatshefte Für Chem. - Chem. Mon.* **2017**, *148*, 3 – 35.

(60) Poelma, S. O.; Burnett, G. L.; Discekici, E. H.; Mattson, K. M.; Treat, N. J.; Luo, Y.; Hudson, Z. M.; Shankel, S. L.; Clark, P. G.; Kramer, J. W.; Hawker, C. J.; Read de Alaniz, J. Chemoselective Radical Dehalogenation and C–C Bond Formation on Aryl Halide Substrates Using Organic Photoredox Catalysts. *J. Org. Chem.* **2016**, *81*, 7155 – 7160.

(61) Ghosh, I.; König, B. Chromoselective Photocatalysis: Controlled Bond Activation through Light-Color Regulation of Redox Potentials. *Angew. Chem. Int. Ed.* **2016**, *55*, 7676 – 7679.

(62) Seo, T.; Kubota, K.; Ito, H. Selective Mechanochemical Monoarylation of Unbiased Dibromoarenes by *in Situ* Crystallization. *J. Am. Chem. Soc.* **2020**, *142*, 9884 – 9889.

(63) Ulrich, G.; Barsella, A.; Boeglin, A.; Niu, S.; Ziessel, R. BODIPY-Bridged Push-Pull Chromophores for Nonlinear Optical Applications. *ChemPhysChem* **2014**, *15*, 2693 – 2700.

(64) Bonnier, C.; Machin, D. D.; Abdi, O.; Koivisto, B. D. Manipulating Non-Innocent π-Spacers: The Challenges of Using 2,6-Disubstituted BODIPY Cores within Donor–Acceptor Light-Harvesting Motifs. *Org. Biomol. Chem.* **2013**, *11*, 3756 – 3760.

(65) Bonardi, L.; Ulrich, G.; Ziessel, R. Tailoring the Properties of Boron−Dipyrromethene Dyes with Acetylenic Functions at the 2,6,8 and 4-B Substitution Positions. *Org. Lett.* **2008**, *10*, 2183 – 2186.

(66) Hayashi, Y.; Yamaguchi, S.; Cha, W. Y.; Kim, D.; Shinokubo, H. Synthesis of Directly Connected BODIPY Oligomers through Suzuki–Miyaura Coupling. *Org. Lett.* **2011**, *13*, 2992 – 2995.

(67) Cakmak, Y.; Akkaya, E. U. Phenylethynyl-BODIPY Oligomers: Bright Dyes and Fluorescent Building Blocks. *Org. Lett.* **2009**, *11*, 85 – 88.

(68) Niu, S.; Ulrich, G.; Retailleau, P.; Ziessel, R. BODIPY-Bridged Push–Pull Chromophores: Optical and Electrochemical Properties. *Tetrahedron Lett.* **2011**, *52*, 4848 – 4853.

(69) Karlsson, J. K. G.; Harriman, A. Origin of the Red-Shifted Optical Spectra Recorded for Aza-BODIPY Dyes. *J. Phys. Chem. A* **2016**, *120*, 2537 – 2546.

(70) Hall, M. J.; McDonnell, S. O.; Killoran, J.; O'Shea, D. F. A Modular Synthesis of Unsymmetrical Tetraarylazadipyrromethenes. *J. Org. Chem.* **2005**, *70*, 5571 – 5578.

(71) Sathyamoorthi, G.; Soong, M.-L.; Ross, T. W.; Boyer, J. H. Fluorescent Tricyclic β-Azavinamidine-BF2 Complexes. *Heteroat. Chem.* **1993**, *4*, 603 – 608.

(72) Adarsh, N.; Avirah, R. R.; Ramaiah, D. Tuning Photosensitized Singlet Oxygen Generation Efficiency of Novel Aza-BODIPY Dyes. *Org. Lett.* **2010**, *12*, 5720 – 5723.

(73) Gorman, A.; Killoran, J.; O'Shea, C.; Kenna, T.; Gallagher, W. M.; O'Shea, D. F. In Vitro Demonstration of the Heavy-Atom Effect for Photodynamic Therapy. *J. Am. Chem. Soc.* **2004**, *126*, 10619 – 10631.

(74) Lin, Z.; Kohn, A. W.; Van Voorhis, T. Toward Prediction of Nonradiative Decay Pathways in Organic Compounds II: Two Internal Conversion Channels in BODIPYs. *J. Phys. Chem. C* **2020**, *124*, 3925 – 3938.

(75) Li, F.; Yang, S. I.; Ciringh, Y.; Seth, J.; Martin, C. H.; Singh, D. L.; Kim, D.; Birge, R. R.; Bocian, D. F.; Holten, D.; Lindsey, J. S. Design, Synthesis, and Photodynamics of Light-Harvesting Arrays Comprised of a Porphyrin and One, Two, or Eight Boron-Dipyrrin Accessory Pigments. *J. Am. Chem. Soc.* **1998**, *120*, 10001 – 10017.

(76) Bahaidarah, E.; Harriman, A.; Stachelek, P.; Rihn, S.; Heyer, E.; Ziessel, R. Fluorescent Molecular Rotors Based on the BODIPY Motif: Effect of Remote Substituents. *Photochem. Photobiol. Sci.* **2014**, *13*, 1397 – 1401.

(77) Lou, Z.; Hou, Y.; Chen, K.; Zhao, J.; Ji, S.; Zhong, F.; Dede, Y.; Dick, B. Different Quenching Effect of Intramolecular Rotation on the Singlet and Triplet Excited States of Bodipy. *J. Phys. Chem. C* **2018**, *122*, 185 – 193.

(78) Karanjit, S.; Kashihara, M.; Nakayama, A.; Shrestha, L. K.; Ariga, K.; Namba, K. Highly Active and Reusable Hydrotalcite-Supported Pd(0) Catalyst for Suzuki Coupling Reactions of Aryl Bromides and Chlorides. *Tetrahedron* **2018**, *74*, 948 – 954.

(79) Welin, E. R.; Le, C.; Arias-Rotondo, D. M.; McCusker, J. K.; MacMillan, D. W. C. Photosensitized, Energy Transfer-Mediated Organometallic Catalysis through Electronically Excited Nickel(II). *Science* **2017**, *355*, 380 – 385.

TOC graphic

substitute photoexcitation for selectivity